Long intergenic non-protein coding RNA-467 targets microRNA-451a in human colorectal cancer

YANG BAI[1,2*], HAIYAN WU[1*], BIN HAN[1], KE XU[1], YUANQI LIU[1], YIN LIU[1], SHIKUN MIAO[1], YUANYUAN ZHANG[1] and LIMING ZHOU[1]

[1]Department of Pharmacology, West China School of Basic Medical Sciences and Forensic Medicine, Sichuan University; [2]Department of Pharmacy, West China Hospital, Sichuan University, Chengdu, Sichuan 610041, P.R. China

Received January 3, 2020; Accepted July 13, 2020

DOI: 10.3892/ol.2020.11987

Abstract. Accumulating evidence has demonstrated that long non-coding RNAs (lncRNAs) are frequently overexpressed in colorectal cancer (CRC). However, few related lncRNA signatures have been established for predicting CRC metastasis. The purpose of the present study was to identify lncRNAs that serve key roles in the metastasis of human CRC, and their potential downstream targets. A total of 31 human CRC biopsy samples were collected, and the expression of long intergenic non-protein coding RNA-467 (linc00467) and its association with clinical characteristics were evaluated. Consequently, linc00467 was revealed to be overexpressed in human CRC tissues, and its expression was significantly associated with metastasis and Tumor-Node-Metastasis stage. In HT29 and HCT116 cells, linc00467-knockout was revealed to decrease cellular proliferation and increase apoptosis ($P<0.05$). Finally, the downstream target of linc00467 in CRC promotion was predicted using bioinformatics analysis. The results demonstrated that linc00467 targets and regulates the expression of microRNA (miR)-451a, promoting carcinogenesis and metastasis in CRC. In conclusion, the results of the present study indicate that increased linc00467 expression promotes metastasis by targeting miR-451a, which ultimately increases cellular proliferation and inhibits apoptosis in human CRC cells.

Correspondence to: Professor Liming Zhou or Professor Yuanyuan Zhang, Department of Pharmacology, West China School of Basic Medical Sciences and Forensic Medicine, Sichuan University, 17 People's South Road, Chengdu, Sichuan 610041, P.R. China
E-mail: zhou108@163.com
E-mail: sarahyyzhang@hotmail.com

*Contributed equally

Key words: linc00467, miR451a, apoptosis, colorectal cancer, metastasis

Introduction

With the third highest global incidence rate among all malignancies (1), colorectal cancer (CRC) continues to pose significant diagnostic, prognostic and therapeutic challenges for clinicians. However, it can be difficult to accurately predict metastasis in patients undergoing curative surgery for localized CRC.

Currently, the dysregulation of functional long non-coding RNAs (lncRNAs) and their involvement in human cancers are receiving considerable attention (2-5); lncRNAs are mRNA-like transcripts ranging from 200 nucleotides to ~100 kilobases in length that lack significant protein-coding ability (6). Accumulating evidence suggests that lncRNAs modulate various cellular functions, and regulate gene expression in several ways, including epigenetic modification, microRNA (miRNA/miR) sponging and mRNA stabilization (7). Long intergenic non-protein coding RNA-467 (linc00467) is a recently identified lncRNA which has rarely been investigated. The first study of linc00467 identified its carcinogenic roles in neuroblastoma; following linc00467 knockdown, tumor cell proliferation was decreased while apoptosis was enhanced, suggesting that linc00467 may act as a tumor suppressor (8). However, the roles, mechanisms, and potential targets of linc00467 in CRC have yet to be fully elucidated (9). A previous study revealed that miR-451a expression was significantly downregulated in CRC tissues and cell lines, which was also associated with a poor outcome in patients with CRC (10). It was therefore hypothesized that miR-451a may be a potential target of linc00467.

To investigate its involvement in CRC, the expression and potential role of linc00467 was assessed in CRC tissues and cell lines. Bioinformatics analysis was conducted to predict the target of linc00467, which was subsequently confirmed in CRC samples and cell lines.

Materials and methods

Patients and tissue samples. Pairs of CRC and normal paracancerous tissues were surgically resected from 31 patients with CRC in the Department of Gastrointestinal

Surgery, West China Hospital, Sichuan University (Chengdu, China), between May 2010 and September 2011, and immediately stored in liquid nitrogen. The paracancerous tissues were ≥5 cm from the CRC tissues and contained no cancer cells, but usually appeared inflamed and fibrotic. Patients were pathologically diagnosed by two independent pathologists according to the World Health Organization classification (11), and the tumors were staged according to the Tumor-Node-Metastasis (TNM) Classification of Malignant Tumors (12). None of the patients underwent chemotherapy prior to surgical resection. The study protocol was reviewed and approved by the Ethics Committee of Sichuan University (approval no. K2016041), and written informed consent was obtained from all patients.

Cell culture. A total of three CRC cell lines (HCT116, HT29 and SW620) were obtained from the American Type Culture Collection. In addition, a normal colonic epithelial cell line (NCM460) was obtained from the Life Science Institute (http://www.sibs.cas.cn/sycs/) and used as a control. HT29 cell line was characterized by Tsingke Biological Technology (http://www.tsingke.net/shop/) using short tandem repeat (STR) markers. The cells were cultured in Dulbecco's modified Eagle's medium containing 10% foetal bovine serum (Thermo Fisher Scientific, Inc.), 100 U/ml penicillin and 100 μg/ml streptomycin, and maintained at 37˚C in a humidified incubator (5% CO_2).

Reverse transcription-quantitative polymerase chain reaction (RT-qPCR). Total RNA was extracted from patient tissues using TRIzol® reagent (Takara Biotechnology Co., Ltd.), according to the manufacturer's protocol. RNA concentration and purity were determined using the Eppendorf BioPhotometer D30 (Eppendorf, Corporate), and RNA integrity was assessed with 1% denaturing agarose gel electrophoresis. First-strand cDNA was synthesized from 2 μg total RNA using 100 U Moloney murine leukaemia virus reverse transcriptase (Invitrogen; Thermo Fisher Scientific, Inc.), in a 10-μl reaction mixture that also contained 1 μl reverse transcription primers (10 mM each) and 10 U RNase inhibitor. The reverse transcription conditions were as follows: RNA samples and primers were mixed in a certain proportion on the ice and reacted at 65˚C for 5 min. The reverse transcription primers were as follows: miR-451a forward, 5'-ACACTCCAGCTGGGAAACCGTTACCATTAC-3' and reverse, 5'-CTCAACTGGTGTCGTGGAGTCGGCAATTCAGTTGAGCTTACAG-3'; U6 forward, 5'-CTCGCTTCGGCAGCAC-3' and reverse, 5'-AACGCTTCACGAATTTGCG-3'; linc00467 forward, 5'-GCGTAGGCCGGACATTTCTA-3' and reverse, 5'-CCTGCCATGTTGGAAACTGC-3; and GAPDH forward, 5'-AGAAGGCTGGGGCTCATTTGC-3' and reverse, 5'-ACAGTCTTCTGGGTGGCAGTG-3'. qPCR was conducted using the AceQ qPCR SYBR Green Master Mix (Vazyme Biotech Co.) in a final volume of 20 μl, containing 10 μl master mix, 0.4 μl each of forward and reverse primer (10 μM) and 2 μl cDNA. The thermocycling conditions were as follows: An initial heating step at 95˚C for 5 min, followed by 35 cycles of 10 sec at 95˚C, and 60˚C for 30 sec. miR-451a and linc00467 expression were normalized to that of the internal U6 and GAPDH controls, respectively. Each sample was run in triplicate and the threshold cycle (Ct) numbers were averaged. Melting curve analysis was performed using the CFX96 Touch™ qPCR System (Bio-Rad Laboratories, Inc.) by increasing the temperature from 65˚C to 95˚C in 0.1˚C/sec increments for each fluorescence reading. Expression level fold-changes were calculated using the relative quantification ($2^{-\Delta\Delta Cq}$) method (13).

Expression vector construction and transfection. A hsa-linc00467-containing region was amplified from human genomic DNA and inserted into pHBcas9n+puro (Hanbio Biotechnology Co., Ltd., Shanghai, China); the linc00467 region was obtained using Zhang Feng's CRISPR gRNA design tool (http://crispr.mit.edu/). The primer sequences were as follows: Forward, 5'-CACCGGGTCTTCGAGAAGACCT-3' and reverse, 5'-AAACAGGTCTTCTCGAAGACCC-3'. Position 113 and 577 of the hsa-linc00467-containing regions were amplified from human genomic DNA and inserted into pSicheck 2.0 (Sinasun Company, Beijing, China; https://sinasun.biomart.cn/), and the corresponding primer sequences were as follows: 113 Forward, 5'-CCGCTCGAGGCGCTGTGACGTTC-3' and reverse, 5'-ATTTGCGGCCGCCCTGTTTGGTCCG-3'; and 577 forward, 5'-CCGCTCGAGAGAGGGACTGAAACTGGG-3' and reverse, 5'-ATTTGCGGCCGCCTCCGCATCCTTCTTTGG-3'. A has-miR451a-containing region was also amplified from human genomic DNA and inserted into pCDNA-3.0 (Hanbio Biotechnology Co., Ltd.), and the primer sequences were as follows: Forward, 5'-CGCGGATCCAGCCTGACAAGGACAGG-3' and reverse, 5'-CCGCTCGAGCCCACCCCTGCCTTGTTTG-3'. Transfection was performed using Lipofectamine® 3000 reagent according to the manufacturer's protocol (Invitrogen; Thermo Fisher Scientific, Inc.). Plasmid concentration and purity were determined using the Eppendorf BioPhotometer D30 (Eppendorf, Corporate). In cellular proliferation assay, each well was transfected with 100 ng plasmid and subsequent experiments were performed 24 h post-transfection. In flow cytometric detection of apoptosis, 2,500 ng plasmid was added to each well and subsequent experiments were performed 48 h post-transfection. In the dual-luciferase assay, 400 ng plasmid was added to each well and subsequent experiments were performed 48 h post-transfection.

Cellular proliferation assay. Cellular proliferation was assessed using a 3-(4, 5-dimethylthiazole-2-yl)-2, 5-diphenyltetrazolium bromide (MTT) assay. Lentivirus-infected cells were seeded into 96-well plates at a density of $2x10^3$ cells per well, and cultured for 24, 48 or 72 h. Next, 20 μl MTT solution was added to each well and the cells were incubated for a further 4 h until a purple precipitate was visible. For each well, 150 μl dimethyl sulfoxide was added to dissolve the purple precipitate and oscillated away from light for 5 min. The spectrophotometric absorbance of each well (at 490 nm) was measured at different time points using a microplate reader absorbance test plate (Molecular Devices). The experimental results were calculated based on the following formula: Inhibition ratio=$(1-A_{pHBcas9n\text{-}linc\ 00467}/A_{pHBcas9n\text{-}NC})$.

Flow cytometric detection of apoptosis. Following transfection with pHBcas9n-linc00467 or pHBcas9n-NC for

48 h, ~1x10^6 cells were collected for apoptosis analysis. Annexin V-FITC solution (5 μl; Vazyme Biotech Co., Ltd.) was added to each sample and gently mixed, and the cells were incubated at room temperature for 10 min in the dark; 10 min before analysis, 5 μl propidium iodide staining solution was added, followed by 4005 μl binding buffer, and the cells were flow cytometrically analyzed (DxFLEX; Beckman Coulter, Inc.). Data for early and late apoptosis are all included.

Dual-luciferase assay. 293T cells were seeded into a 24-well plate (5x10^4 per well) and transfected with 200 ng psiCheck2-NC (Sinasun Company, Beijing, China)+pCDNA-miR451a (Hanbio Biotechnology Co., Ltd.), psiCheck2-113+pCDNA-miR451a or psiCheck2-577+pCDNA-miR451a using Lipofectamine® 3000 (Invitrogen; Thermo Fisher Scientific, Inc.). The 3'UTR region of linc00467 was amplified and inserted into the plasmid with the following primers: 113 Forward 5'-CCGCTCGAGGCG CTGTGACGTTC-3' and reverse, 5'-ATTTGCGGCCGCCCT GTTTGGTCCG-3'. 577 forward 5'-CCGCTCGAGAGAGGG ACTGAAACTGGG-3' and reverse, 5'-ATTTGCGGCCGC CTCCGCATCCTTCTTTGG-3'. After a 48-h incubation period, cell lysates were collected to assess Firefly and *Renilla* luciferase activities using the Dual-Luciferase reporter system (Promega Corporation).

Bioinformatics analysis. The potential binding sites between linc00467 and miR-451a were predicted by uploading their sequences to the online software RNAhybrid (https://bibiserv.cebitec.uni-bielefeld.de/rnahybrid?id=rnahybrid_view_submission). A total of 10 potential binding sites were predicted, and the top 2 sites were selected for further investigation.

Statistical analysis. All data are expressed as the mean ± standard deviation. Relative gene expression was analysed using the Livak and Schmittgen method (13). Differences between groups were determined using the Student's t-test or analysis of variance, followed by Tukey's post hoc test. The non-parametric Wilcoxon-Mann-Whitney or Kruskal-Wallis tests were used to analyse the association between the linc00467 expression level and various clinico-pathological characteristics. P<0.05 was considered to indicate a statistically significant difference.

Results

The expression of linc00467 is upregulated and is associated with TNM stage and serum carcinoembryonic antigen (CEA) level in CRC. Of the 31 patients included in the present study, 15 were males and 16 were females, and all were aged between 30 and 90 years. As shown in Table I and Fig. 1, compared with paracancerous tissues from the same patients, linc00467 was overexpressed in >60% of the 31 CRC specimens, with an average increase of 1.75 times the expression level in paracancerous tissues. Furthermore, linc00467 expression was significantly associated with metastasis (P<0.05) and an advanced clinical stage of CRC (P<0.05). In cases with lymph node metastasis, linc00467 was overexpressed in 92% (11/12) of patients. However, linc00467 was overexpressed in only 32% (6/19) of patients without lymph node metastasis. Furthermore, linc00467 was overexpressed in only 40% (8/20) of patients with serum CEA ≤3.4 ng/ml, but in 82% (9/11) of patients with a CEA level >3.4 ng/ml.

Table I. Association between linc00467 expression and pathological features in patients with CRC.

Variable	N (%)	Median linc00467 expression	P-value
Age, years			0.64
≤58	15 (48.39)	2.11	
>58	16 (51.61)	3.08	
Sex			0.40
Male	16 (51.61)	3.10	
Female	15 (48.39)	2.08	
Differentiation			0.44
Poor	4 (12.90)	4.62	
Moderate	27 (87.10)	2.31	
CEA, ng/ml			<0.01[a]
≤3.4	20 (64.52)	1.62	
>3.4	11 (35.48)	4.41	
Lymphatic metastasis			<0.01[a]
Yes	12 (38.71)	5.65	
No	19 (61.29)	0.69	
T-stage			0.16
T2	8 (25.81)	0.79	
T3	6 (19.35)	2.59	
T4	17 (54.84)	3.32	
Clinical stage			<0.01[a]
I+II	18 (58.06)	0.44	
III+IV	13 (41.94)	5.01	

[a]P<0.01. Quantified by quantitative polymerase chain reaction. linc00467 was normalized to GAPDH. Mann-Whitney test was used to compare between two groups and Kruskal-Wallis test was used to compare between more than two groups.

Knocking out linc00467 inhibits the proliferation of CRC cells. As shown in Fig. 2A, the relative expression levels of linc00467 in HCT116, HT29 and SW620 cells were 3.26-, 5.94- and 2.24-fold, respectively, compared with that in NCM460 cells. HCT116 and HT29 cells were transfected with pHBcas9n-lin00467 or pHBcas9n-NC plasmids for 24 h using Lipofectamine® 3000 reagent. As shown in Fig. 2B, linc00467-knockout decreased the proliferation of HCT116 and HT29 cells by 90.87 and 71.84%, respectively. The inhibitory effects on proliferation were evident at 24 h, but most apparent at 72 h post-transfection (Fig. 2C). The PHBcas9n-lin00467 plasmid was completely sequenced following construction; a peak in the linc00467 insertion sequence fragment indicates that construction of the target gene knockout plasmid was successful (Fig. 2D and E).

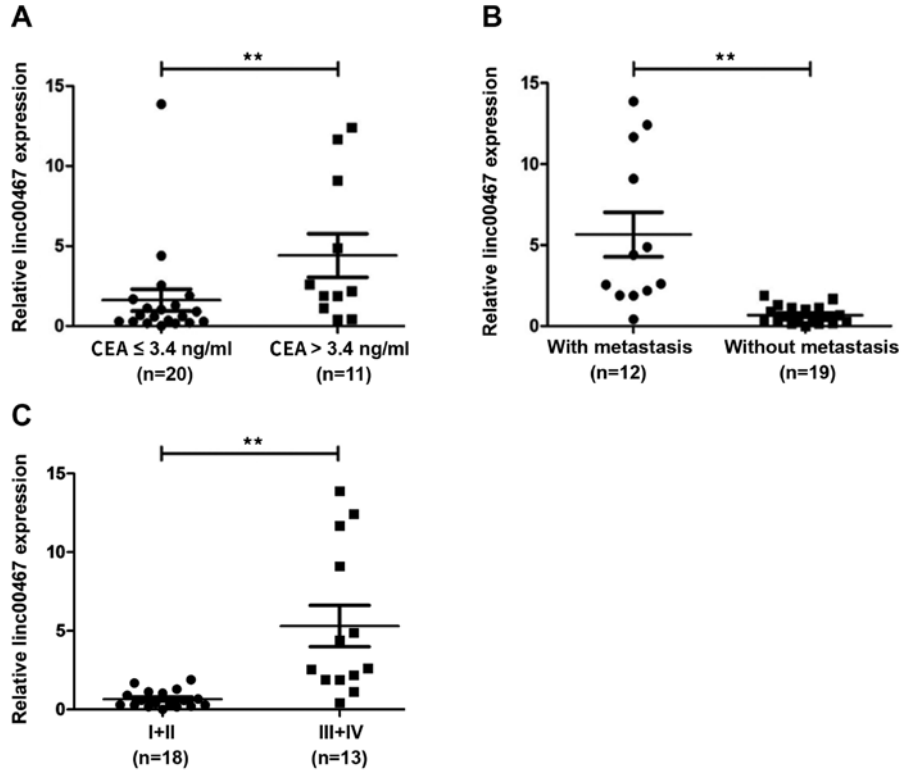

Figure 1. The association between linc00467 expression and clinical characteristics of patient samples. (A) Association between linc00467 expression level and patients' carcinoembryonic antigen (CEA) level (**P<0.01). (B) Association between presence of lymph node metastasis and lin00467 expression (**P<0.01). (C) Association between linc00467 expression level and different clinical stages (I+II, III+IV stages) (**P<0.01).

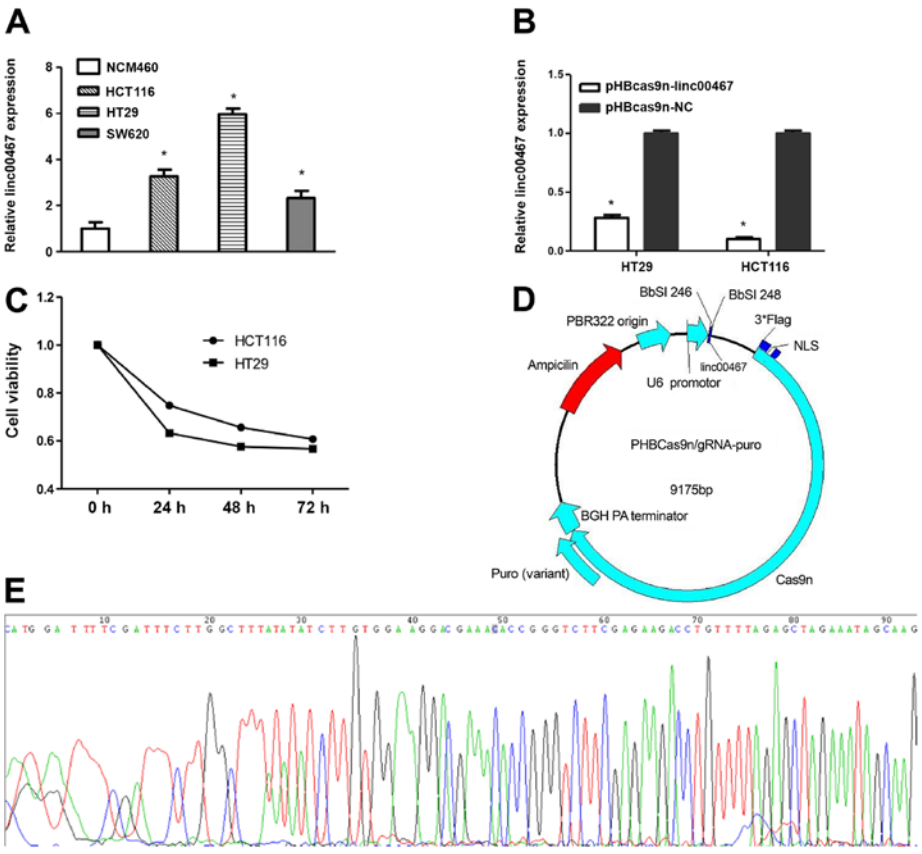

Figure 2. Relative expression of linc00467 in NCM460, HCT116, HT29, and SW620 cells was determined by quantitative polymerase chain reaction, compared with GAPDH. (A) Compared with NCM460 cells, linc00467 was highly expressed in HCT116 and HT29 CRC cell lines. (B) Knocking out linc00467 inhibited the proliferation of CRC cells. (C) The effects on cell proliferation of HCT116 and HT29 following linc00467-knockout. (D) The map of plasmid pHBcas9n-lin00467. (E) Sequencing linc00467 insert fragment. *P<0.05.

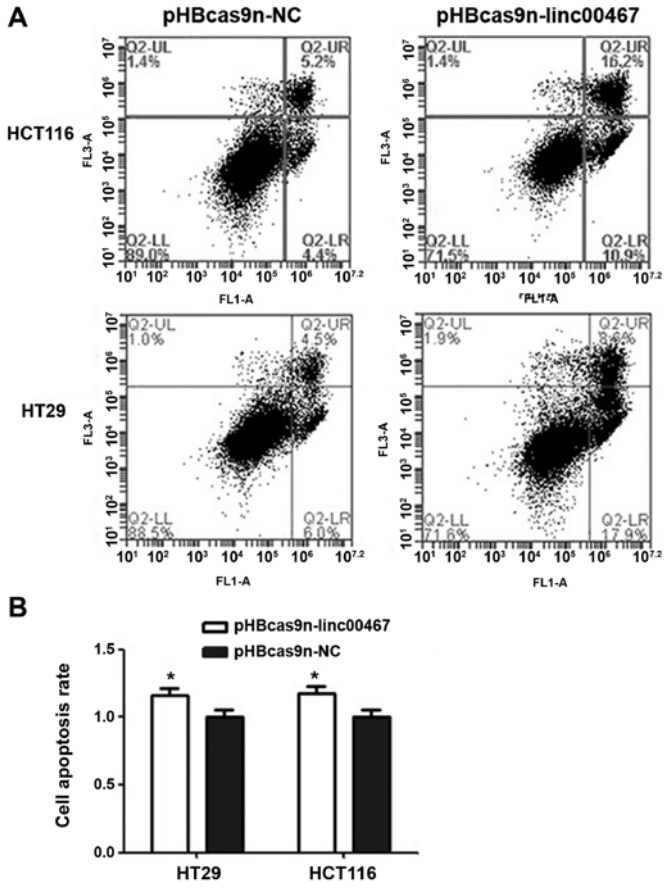

Figure 3. (A) Using flow cytometry to assess the percentage of apoptotic cells 48 h after transfection. Representative scatter plots and quantitative results are shown. (B) Relative apoptosis rates of HT29 and HCT116 cells following linc00467-knockout (n=3; *P<0.05).

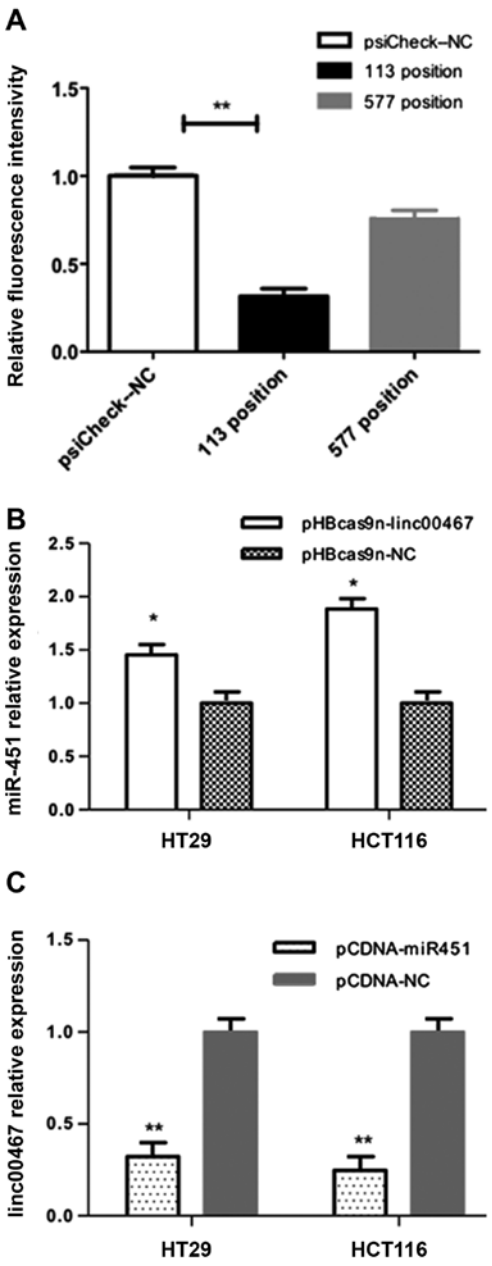

Figure 4. (A) Bioinformatics prediction of binding sites between miR-451a and linc00467. (B) The expression of miR-451a in CRC cells following linc00467-knockout. (C) Overexpression of miR-451a in CRC cells can reduce the cellular linc00467 content. *P<0.05 and **P<0.01.

Knocking out linc00467 induces apoptosis in CRC cells. Following linc00467-knockout, HCT116 cell apoptosis was increased by 17.5% compared with the pHBcas9n-NC plasmid control group (Fig. 3A and B). The number of cells undergoing early apoptosis was increased by 6.5%, while the number of those in late apoptosis increased by 11%. HT29 cell apoptosis was increased by 16% following linc00467-knockout. The number of early and late apoptotic cells increased by 11.9 and 4.1%, respectively, compared with those in the pHBcas9n-NC group.

linc00467 binds miR-451a as an endogenous competitor. Bioinformatics analysis predicted that miR-451a was a potential target of linc00467, with several possible binding sites. Positions 113 and 577 were the most likely binding sites since they generated the highest predictive scores (RNAhybrid online software). Compared with the pSicheck2-NC+pCDNA-miR451a group, the fluorescence intensity of the psiCheck2-577+pCDNA-miR451a group was only decreased to 75.83%, while that of the psiCheck2-113+pCDNA-miR451a group was decreased to 31.62% (Fig. 4A; P<0.01).

HT29 and HCT116 cells were transfected with pHBcas9n-lin00467 for 48 h, and miR-451a expression was quantified by RT-qPCR. In HT29 cells, the expression level of miR-451a was 1.45-fold higher in the pHBcas9n-lin00467 group (P<0.05) than in the pHBcas9n-NC group. In HCT116 cells, miR-451a expression was 1.88-fold higher in the pHBcas9n-lin00467 group compared with the pHBcas9n-NC group (Fig. 4B).

HT29 and HCT116 cells were transfected with pCDNA-miR451a for 48 h, and the expression level of linc00467 was subsequently determined. In HT29 cells, linc00467 expression was reduced by 68% in the pCDNA-miR451a group, compared with the pCDNA-NC group. In HCT116 cells, linc00467 expression in the pCDNA-miR451a group was decreased by 76% compared with the pCDNA-NC group. These findings indicate that miR451a overexpression decreases the level of linc00467 in CRC cells (Fig. 4C).

Discussion

The results of the present study suggest that linc00467 may be a suitable predictor of CRC metastasis, as its expression was revealed to be associated with lymph node metastasis in patients with CRC. In addition, linc00467 expression in CRC was revealed to be associated with the serum CEA level, and its expression in CRC cell lines was significantly higher than that in normal colorectal epithelial cells, which was consistent with the results in human CRC specimens.

To the best of our knowledge, our previous study was the first to illustrate that miR-451a expression was decreased in CRC tissues, and that it may act as a tumor suppressor (10). It was also indicated that miR-451a and linc00467 were expressed to differing degrees in CRC, which was consistent with the characteristics of the competing endogenous (ceRNA) theory (12,14). The ceRNA theory hypothesizes that the combination of miRNA and mRNA can inactivate a target gene and decrease the expression of miRNA (15,16). The results of the present study confirm that linc00467 overexpression in CRC leads to the downregulation and antagonism of miR-451a. As a tumor-suppressor, the function of miR-451a was abolished by the overexpression of linc00467.

The potential targets of miR-451a and linc00467 were evaluated with RNAhybrid using the miRNA response element (MRE) of linc00467 (17,18). Following bioinformatics prediction, two binding sites with the highest scores among the potential MREs were selected, namely positions 113 and 577. A luciferase assay directly demonstrated that linc00467 possesses a binding site for miR451a, which is a target gene directly regulated via linc00467 locus 113.

The present findings are also supported by other studies. For example, in CRC, H19 can promote epithelial-mesenchymal transition by functioning as an miR-138 and miR200a sponge (19). Furthermore, lncRNA-ROR promotes proliferation, invasiveness and metastasis by associating with miR-145 (20). The current results suggest that linc00467 is upregulated in CRC tissues and as an endogenous competitor, downregulates miR-451a expression, which subsequently regulates a variety of downstream oncogenes to promote CRC metastasis.

In conclusion, the present study demonstrates that linc00467 is upregulated in CRC, and that knocking out linc00467 can inhibit the proliferation of CRC cells and induce apoptosis. Additionally, as a novel tumor suppressor in CRC, miR-451a was found to be downregulated and associated with TNM stage and distant metastasis in CRC. As an endogenous competitive RNA molecule, linc00467 binds to miR-451a and subsequently regulates the expression of tumor suppressive factors in CRC.

Acknowledgements

Not applicable.

Funding

Not applicable.

Availability of data and materials

The datasets used and analyzed during the present study are available from the corresponding author upon reasonable request.

Authors' contributions

YB and HW designed and conducted the study and wrote the manuscript. BH, KX and YQL conducted the study and helped to write the manuscript. YL and SM helped to analyze the data. YZ and LZ conceived and designed the study. All authors reviewed and approved the final version of the manuscript.

Ethics approval and consent to participate

The study protocol was reviewed and approved by the Ethics Committee of Sichuan University (no. K2016041).

Patient consent for publication

Written informed consent was obtained from patients prior to sampling.

Competing interests

The authors declare that they have no competing interests.

References

1. Ferlay J, Shin HR, Bray F, Forman D, Mathers C and Parkin DM: Estimates of worldwide burden of cancer in 2008: GLOBOCAN 2008. Int J Cancer 127: 2893-2917, 2010.
2. Gibb EA, Brown CJ and Lam WL: The functional role of long non-coding RNA in human carcinomas. Mol Cancer 10: 38, 2011.
3. Lin C and Yang L: Long noncoding RNA in cancer: Wiring signaling circuitry. Trends Cell Biol 28: 287-301, 2018.
4. Schmitt AM and Chang HY: Long noncoding RNAs in cancer pathways. Cancer Cell 29: 452-463, 2016.
5. Prensner JR and Chinnaiyan AM: The emergence of lncRNAs in cancer biology. Cancer Discov 1: 391-407, 2011.
6. Lipovich L, Johnson R and Lin CY: MacroRNA underdogs in a microRNA world: Evolutionary, regulatory, and biomedical significance of mammalian long non-protein-coding RNA. Biochim Biophys Acta 1799: 597-615, 2010.
7. Batista PJ and Chang HY: Long noncoding RNAs: Cellular address codes in development and disease. Cell 152: 1298-1307, 2013.
8. Atmadibrata B, Liu PY, Sokolowski N, Zhang L, Wong M, Tee AE, Marshall GM and Liu T: The novel long noncoding RNA linc00467 promotes cell survival but is down-regulated by N-Myc. PLoS One 9: e88112, 2014.
9. He X, Li S, Yu B, Kuang G, Wu Y, Zhang M, He Y, Ou C and Cao P: Up-regulation of LINC00467 promotes the tumorigenesis in colorectal cancer. J Cancer 10: 6405-6413, 2019.
10. Xu K, Zhang YY, Han B, Bai Y, Xiong Y, Song Y and Zhou LM: Suppression subtractive hybridization identified differentially expressed genes in colorectal cancer: microRNA-451a as a novel colorectal cancer-related gene. Tumor Biol 39: 1010428317705504, 2017.
11. Jernman J, Välimäki MJ, Louhimo J, Haglund C and Arola J: The novel WHO 2010 classification for gastrointestinal neuroendocrine tumours correlates well with the metastatic potential of rectal neuroendocrine tumours. Neuroendocrinology 4: 317-324, 2012.
12. Hu H, Krasinskas A and Willis J: Perspectives on current tumor-node-metastasis (TNM) staging of cancers of the colon and rectum. Semin Oncol 4: 500-510, 2011.
13. Livak KJ and Schmittgen TD: Analysis of relative gene expression data using real-time quantitative PCR and the 2(-Delta Delta C(T)) method. Methods 25: 402-408, 2001.

14. Salmena L, Poliseno L, Tay Y, Kats L and Pandolfi PP: A ceRNA hypothesis: The rosetta stone of a hidden RNA language? Cell 146: 353-358, 2011.
15. Wapinski O and Chang HY: Corrigendum: Long noncoding RNAs and human disease. Trends Cell Biol 21: 561, 2011.
16. Crick FH, Barnett L, Brenner S and Watts-Tobin RJ: General nature of the genetic code for proteins. Nature 192: 1227-1232, 1961.
17. Bartel DP: MicroRNAs: Target recognition and regulatory functions. Cell 136: 215-233, 2009.
18. Djebali S, Davis CA, Merkel A, Dobin A, Lassmann T, Mortazavi A, Tanzer A, Lagarde J, Lin W, Schlesinger F, *et al*: Landscape of transcription in human cells. Nature 489: 101-108, 2012.
19. Liang WC, Fu WM, Wong CW, Wang Y, Wang WM, Hu GX, Zhang L, Xiao LJ, Wan DC, *et al*: The lncRNA H19 promotes epithelial to mesenchymal transition by functioning as miRNA sponges in colorectal cancer. Oncotarget 6: 22513-22525, 2015.
20. Zhou P, Sun L, Liu D, Liu C and Sun L: Long non-coding RNA lincRNA-ROR promotes the progression of colon cancer and holds prognostic value by associating with miR-145. Pathol Oncolo Res 22: 733-740, 2016.